Journal of Applied Fluid Mechanics, Vol. 16, No. 12, pp. 2518-2528, 2023.
Available online at www.jafmonline.net, ISSN 1735-3572, EISSN 1735-3645.
https://doi.org/10.47176/jafm.16.12.1953

Effect of Personalized Ventilation in Seat Armrest on Diffusion Characteristics of Respiratory Pollutants in Train Carriages

X. Liu, T. Li†, S. Wu, and J. Zhang

State Key Laboratory of Rail Transit Vehicle System, Southwest Jiaotong University, Chengdu, China

†Corresponding Author Email: litian2008@home.swjtu.edu.cn

ABSTRACT

As one of the most important means of transportation, high-speed trains have a large capacity for carrying passengers. However, their narrow carriages can easily exacerbate the spread of respiratory diseases. Just like personalized ventilation in an airplane, ventilation in seat armrests of high-speed trains may increase comfort for passengers, but also influence the diffusion characteristics of respiratory pollutants. In this study, the effect of personalized ventilation in seat armrests, on the diffusion characteristics of respiratory pollutants in train carriages, is studied by means of the tracer gas method. Taking the ceiling air supply as the original ventilation system, comfortable temperature and pollutant diffusion characteristics of the personalized ventilation system, with 4 different air supply angles, are investigated. The 4 angles are 0°, 30°, 45° and 60°. When the personalized ventilation with the above 4 angles is adopted, the fluctuation amplitudes of pollutants in the passenger breathing zone are reduced by 15.84%, 19.27%, 19.76% and 19.68%, respectively, compared with the original ventilation system. It indicates that the sensible use of personalized ventilation can effectively reduce the passengers' contaminant concentrations in the breathing zone, thereby reducing the possibility of cross-contamination between passengers. In addition, the use of the personalized ventilation system leads to a slight improvement in the thermal comfort and flow uniformity in the carriage. Based on the results, personalized air supply with an angle of 45° is advised for use in high-speed trains.

Article History

Received April 20, 2023
Revised August 4, 2023
Accepted August 5, 2023
Available online October 8, 2023

Keywords:

CFD
Indoor air quality
Numerical simulation
Personalized ventilation
Tracer gas

1. INTRODUCTION

A survey has shown that frequent taxi passengers have greater respiratory exposure, and are thus susceptible to respiratory diseases (Hachem et al., 2019). The similarity between train carriages and taxis is that they are both relatively small, enclosed spaces. If the ventilation system is not good, it will endanger the health of passengers, so it is important to study the ventilation systems of train carriages.

Many studies have shown that different ventilation systems and design parameters have a certain impact on aerosol transport and virus diffusion (Liu et al., 2021; Sen 2021; Izadyar & Miller 2022;). In the context of the global epidemic of novel coronary pneumonia, we have investigated a novel approach to air supply and emissions, to reduce the risk of respiratory infections and protect the health of passengers.

Up to now, there have been many studies that have focused on vehicle ventilation systems. Wang et al. (2014) found that there are differences in the ability of different air distribution systems to remove respiratory pollutants in carriages. Zhang & Li (2021) studied the effect of train ventilation on the diffusion of respiratory pollutants. Li et al. (2015) changed the air supply angle and flow rate in the cabin, with the purpose of improving air quality. Indoor respiratory pollutants are easily affected by ventilation. Considering the existing carriage ventilation system, this paper adds the personalized ventilation system, to reduce the diffusion of respiratory pollutants in the carriage. As a new type of ventilation, the personalized ventilation system can control the flow in the local area around a passenger, and has great potential to improve thermal comfort and pollutant diffusion characteristics in enclosed spaces. The research shows that the personalized ventilation system has a certain impact on the passenger environment, and the reasonable use of personalized ventilation systems can improve the ventilation efficiency

NOMENCLATURE

α_H	heat transfer coefficient	$\Gamma_{\phi,\text{eff}}$	effective diffusion coefficient
ε	turbulence dissipation rate	θ	angle
μ	dynamic viscosity	μ_t	turbulent viscosity
ν	kinematics viscosity	ρ	air density
ρ_a	absorption coefficient of the outer surface	ω	train speed
ω_k	angular velocity	*CFD*	Computation Fluid Dynamics
G_k	Generation of turbulent kinetic energy due to the mean velocity gradient	*J*	total radiation intensity
k	Turbulent kinetic energy	k_x	non-uniform coefficient
PV	personalized ventilation	RANS	Reynolds-Averaged Navier-Stokes
t_c	wall temperature of the carriages	t_d	equivalent temperature of solar radiation
t_h	ambient temperature		

and reduce the carbon dioxide concentration in the human breathing area (Mao et al., 2022). There are few practical applications of personalized ventilation, so it is necessary to optimize the design based on the existing knowledge. A lot of research is needed in the future (Melikov, 2004). When a personalized ventilation system is used, different background ventilation has a significant influence on its performance, which may cause problems, such as accelerating the spread of pathogens. However, the results show that the individual ventilation system combined with displacement ventilation can significantly improve the quality of inhaled air. Research on personalized ventilation systems has focused on aircraft cabins, building interiors and other public places, and there are also certain studies in the aerospace field (Razvan et al., 2021). Its performance is mainly affected by factors such as the location of the equipment, the air flow rate, and the size of the air outlet. Zhang et al. (2012) proposed a personalized air supply device combined with upper and lower return, which is embedded in the end of the air duct, in the armrest of an aircraft seat. It can effectively meet the requirements of human thermal comfort. Mboreha et al. (2022) designed six kinds of personalized ventilation systems for use in the cabin of an airplane. By comparing the distribution of pollutants in the cabin, the best design scheme was selected. Melikov et al. (2012) arranged personalized ventilation at the seat headrest, which could improve the quality of the inhaled air and reduce the risk of air cross-infection. Ghaddar et al. (2021) developed an autonomously controlled personalized ventilation system, in order to meet thermal comfort requirements under steady-state and transient indoor conditions. However, when the personalized ventilation system is used in unsuitable circumstances, it may increase human discomfort and the probability of disease transmission (Xui et al., 2021). Elvire et al. (2021) studied the effect of indoor personalized ventilation on cross-infection, and the results showed that when only one set of personalized ventilation system was used, the diffusion of pollutants was not effectively alleviated. Xu et al. (2020) found that personalized ventilation can reduce the probability of infection, by increasing the amount of fresh air in the breathing zone of the human body. When an infected person uses a personalized ventilation system, however, it may accelerate the mixing of the virus with the air and increase the probability of infection of susceptible people. Looking at personalized ventilation system optimization, Alain et al. (2015) proposed a new type of coaxial nozzle personalized ventilation system that can effectively improve the human breathing area air quality. Xu et al. (2018) studied the interaction between personalized ventilation and human requirements, to design the best ventilation scheme. Assaad et al. (2019) used an office model to study the effect of airflow generated by exercise, done while using personalized ventilation. The study showed that airflow generated by exercise would affect the function of a personalized ventilation system. When the distance between people is 85cm, the inhaled air quality can be effectively improved. Xu et al. (2021) studied the influence of air flow distance on the performance of personalized ventilation systems, and concluded that reasonable distance can make the systems' performance better.

Respiratory pollutants are expelled from the body in the form of droplets, which are then evaporated and settle on solid surfaces, or are inhaled by others. The papers show that the evaporation and deposition of the droplets are mainly related to the ambient humidity and the diameter of the droplets (Wei & Li, 2015; Li et al., 2018). At present, Computational Fluid Dynamics (CFD) is widely used in the field of mass transfer, and the tracer gas method is mainly used in the study of the diffusion of respiratory pollutants. This method does not need to consider the evaporation of droplets (Debnath et al., 2018). The principle of the tracer gas method (Sherman, 1990) is to use CO_2 or other tracers to replace the droplet core, and to predict the trajectory of the tracer, which can effectively avoid some limitations of particle simulation (Ai et al., 2020). Li et al. (2011, 2013) studied the transmission law of human exhaled droplets under different ventilation methods and different particle sizes, and the results showed that the distribution of particles with smaller particle sizes was similar to the distribution of tracer gases.

Numerical simulation using the tracer gas method has high accuracy, since the particles exhaled by the human body are all particles of small particle size. Thus, the tracer gas method can be used for research. In this paper, CO_2 is used as a tracer, to study the diffusion characteristics of pollutants breathed by passengers.

Due to the closed environment of the train carriage, which creates conditions conducive to the spread of various respiratory pollutants (Mangili & Gendreav,

2005), mixed ventilation and displacement ventilation may not guarantee the health of passengers. After adding personalized ventilation, the probability of virus infection can be reduced to a certain extent, and people can travel normally. In this paper, the ceiling ventilation system is used as background ventilation and the terminal of the personalized ventilation system is positioned in the armrest. This study compares the distribution of flow field, temperature and respiratory pollutants around typical passengers with this ventilation at 0 °, 30 °, 45 ° and 60 ° air supply angles.

2. MATHEMATICAL MODEL AND EVALUATION INDICATORS

2.1 Turbulence Model

Indoor airflow is a low-speed turbulent flow, and the indoor flow field can be obtained by solving the RANS equation. The transport equation is as follows

$$\frac{\partial}{\partial t}(\rho\phi)+\frac{\partial}{\partial x_j}(\rho u_j\phi)=\frac{\partial}{\partial x_j}(\Gamma_{\phi,eff}\frac{\partial\phi}{\partial x_j})+S_\phi \tag{1}$$

where ρ is the air density, u_j is the velocity component, ϕ is a scalar variable (This variable will be changed when the tracer gas concentration equation is expressed), $\Gamma_{\phi,eff}$ is the effective diffusion coefficient and S_ϕ is the source term. At present, there are many types of turbulence models, and the LES method and *k*-□ model are often used in the study of indoor air flow (Chen, 1995; Pesic et al., 2016). The realizable *k*-□ model is often used to study air flow in train compartments (Li et al. 2022). Therefore, the realizable *k*-□ model will be used in this paper**.** The transport equation is as follows

$$\frac{\partial(\rho k)}{\partial t}+\frac{\partial(\rho k u_i)}{\partial x_i}=\frac{\partial}{\partial x_j}\left[\left(\mu+\frac{\mu_t}{\sigma_k}\right)\frac{\partial k}{\partial x_j}\right]+G_k-\rho\varepsilon \tag{2}$$

$$\frac{\partial(\rho\varepsilon)}{\partial t}+\frac{\partial(\rho\varepsilon u_i)}{\partial x_i}=\frac{\partial}{\partial x_j}\left[\left(\mu+\frac{\mu_t}{\sigma_k}\right)\frac{\partial\varepsilon}{\partial x_j}\right]+\rho\varepsilon C_1E-\rho C_2\frac{\varepsilon^2}{k+\sqrt{\nu\varepsilon}} \tag{3}$$

in Eq. (2) and Eq. (3), σ_k, C_2 and σ_ε are constants (Shih et al., 1995), $\sigma_k=1.0$, $C_2=1.9$, $\sigma_\varepsilon=1.2$, $C_1=\max(0.43,\frac{\eta}{\eta+5})$, $\eta=(2E_{ij}\cdot E_{ij})^{1/2}\frac{k}{\varepsilon}$, $E=\sqrt{2E_{ij}E_{ij}}$, E is the strain rate, $E_{ij}=\frac{1}{2}(\frac{\partial u_i}{\partial x_j}+\frac{\partial u_j}{\partial x_i})$, u_t and C_μ are calculated according to the following formula

$$\mu_t=\rho C_\mu\frac{k^2}{\varepsilon} \tag{4}$$

$$C_\mu=\frac{1}{A_0+\left[\sqrt{6}k\cos(\frac{1}{3}\cos^{-1}(\sqrt{6}\frac{E_{ij}E_{jk}E_{kj}}{(E_{ij}E_{ij})^{1/2}}))\sqrt{E_{ij}E_{ij}+\tilde{\Omega}_{ij}\tilde{\Omega}_{ij}}\right]/\varepsilon} \tag{5}$$

in Eq. (5), A_0 are constants, $A_0=4.0$, $\tilde{\Omega}_{ij}=\Omega_{ij}-2\varepsilon_{ijk}\omega_k$, $\Omega_{ij}=\bar{\Omega}_{ij}-\varepsilon_{ijk}\omega_k$, $\bar{\Omega}_{ij}$ is the mean rate of rotation tensor viewed in a moving reference frame with the angular velocity.

2.2 Mean Non-Uniform Coefficient

In this study, the mean non-uniform coefficient is used as the evaluation indicator of thermal comfort of passengers in the carriages. The larger the mean non-uniform coefficient, the greater the fluctuation of the flow field in the vehicle, and the worse the thermal comfort of the journey. The calculation formula is as follows

$$k_x=\frac{\sigma_x}{\bar{x}} \tag{6}$$

$$\bar{x}=\frac{\sum x_i}{n} \tag{7}$$

$$\sigma_x=\sqrt{\frac{\sum(x_i-\bar{x})^2}{n}} \tag{8}$$

where k_x is the mean non-uniform coefficient, x_i is the velocity or temperature at the sampling point, $\bar{x}$ is the average value of the velocity or temperature, σ_x is the root mean square deviation.

3. COMPUTATIONAL MODEL

3.1 Carriage Model

In order to study the influence of the personalized ventilation system of the train on respiratory pollutants, a carriage model was established (18377×3000×2400 mm). When the carriage model is established, we take the direct contact air wall as the car body. We don't consider the small structures of the carriage, or windows and doors, and simplify a human body and seat as a box. As shown in Fig. 1, the calculation adopts the full load condition, and there are a total of 90 seats in the carriage, consisting of 18 rows of 5 seats. The outlet is set at the lower part of the luggage rack on both sides, with a single size of 18377×100 mm, and is used as the ceiling air supply. Personalized vents are arranged on the insides of the armrests of each seat, all of a single size of 100×50 mm.

The passengers in the ninth row were taken as the research object, and nine planes of 0.3 × 0.3 m were taken in the breathing area of the five passengers. The average CO_2 concentration of the nine planes was used as the CO_2 concentration of the passenger breathing area. As shown in Fig 1(b), four monitoring lines were set up, at the legs, armrests, head and above the passengers in the ninth row, to monitor the air velocity and temperature in the train compartment. The height of the four monitoring lines from the ground were 0.1 m, 0.7 m, 1.3 m and 1.7 m, respectively.

3.2 Boundary Conditions

The train is affected by the ambient temperature and solar radiation when running, which will indirectly affect the distribution of the infield in the carriage (Barone et al., 2020). The calculation formula of the body wall temperature is as follows

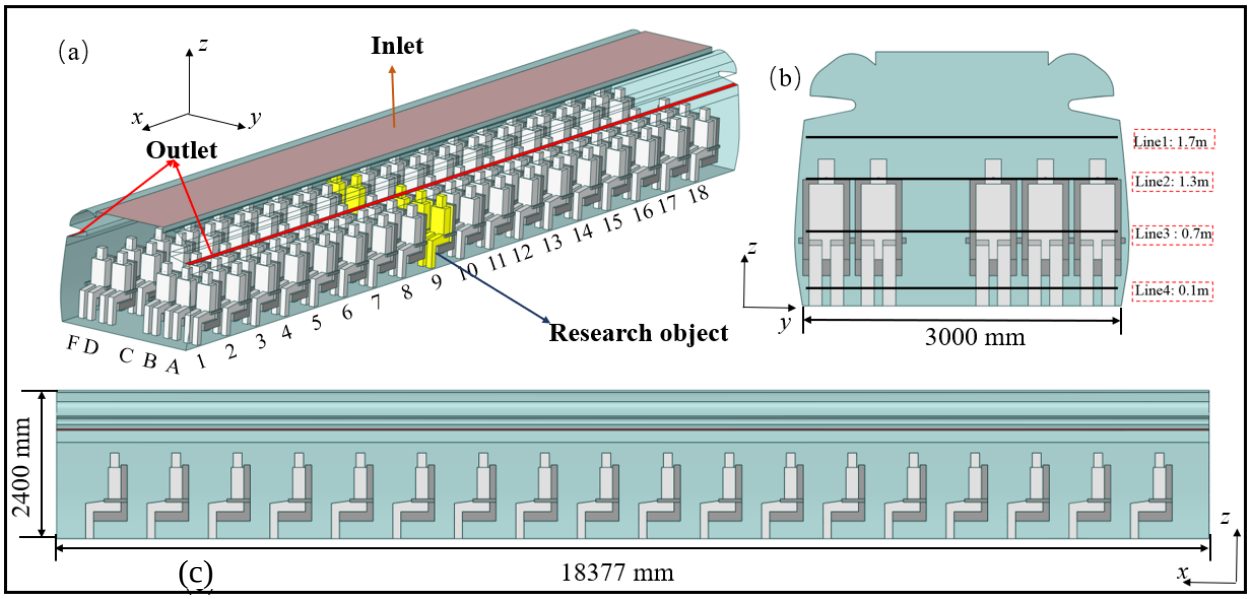

Fig. 1 Model (a) Carriage model; (b) Monitoring line location; (c) Size of the model

Table 1 Air supply case.

Case	Personalized ventilation
Case 1	Doesn't use a personalized ventilation system
Case 2	Personalized ventilation angle is 0° from horizontal
Case 3	Personalized ventilation angle is 30° from horizontal
Case 4	Personalized ventilation angle is 45° from horizontal
Case 5	Personalized ventilation angle is 60° from horizontal

$$t_c = t_h + t_d = t_h + \frac{\rho_a J}{\alpha_H} \tag{9}$$

$$\alpha_H = 9 + 8.155\omega^{0.66} \tag{10}$$

where t_c is the wall temperature of the carriages, t_h is the ambient temperature; t_d is the equivalent temperature of solar radiation, ρ_a is the absorption coefficient of the outer surface of the vehicle, taken as 0.5, J is the total radiation intensity, W/m^2, α_H is the heat transfer coefficient of the outer surface of the vehicle, W/(m^2•K). ω is the running speed of the train, in m/s. In this study, ω=69.44m/s. The working conditions studied in this paper are summer working conditions, and the ambient temperature is assumed to be 35 °C. According to formulae (9) and (10), the body wall temperature is 37.45°C.

All passengers in the car are considered to have an exhalation process. According to Gupta's research, the exhalation speed of passengers is set to 2.24 m/s (Gupta et al., 2009, 2010), at 60° from the horizontal direction, with an airflow temperature of 32°C. CO_2 is used as the tracer gas for passenger breathing pollutants, and the proportion of CO_2 is 100%. At the same time, the human body surface temperature can be set to 32°C (Yang et al., 2015). The air in the carriage conforms to the Boussinesq assumption (Zhou et al., 2018; Mechighel et al., 2021). The effect of gravity is considered in the simulation and the air tightness of the carriages is good (Wu et al. 2022).

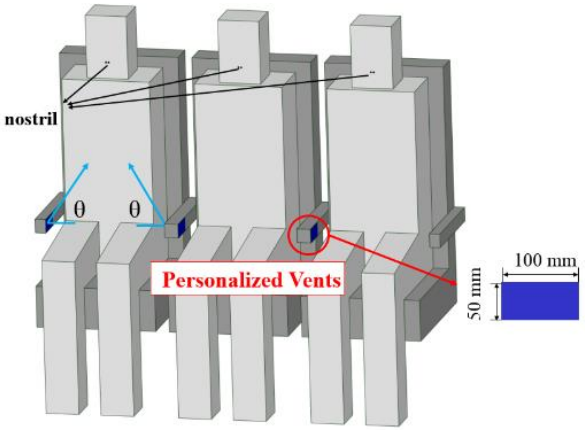

Fig. 2 Personalized ventilation system

This paper proposes four personalized ventilation cases and a no personalized ventilation case. Personalized vents are arranged on the inside of the armrests of each seat, each with a single size of 100×50 mm. Figure 2 details the personalized ventilation system, θ is the angle between the airflow and the horizontal direction, which is 0°, 30°, 45°, and 60°, respectively. The boundary conditions are shown in Table 2.

3.3 Grid Independence Test

In order to improve the calculation efficiency, a grid independence test was carried out. First, three sets of polyhedral meshes were divided by Fluent meshing, with numbers of about 7.18 million, 12.80 million, and 18.09

Table 2 Boundary condition

Items	Values	Items	Values
Air supply flow rate	4800 m^3/h	Seat	Adiabatic
Air supply temperature	17℃	Body surface temperature	32℃
Heat transfer coefficient	1.2 $W/(m^2 \cdot K)$	Both ends of the carriage	Symmetry
PV air supply wind speed	0.3 m/s	Luggage rack	Adiabatic
PV air supply temperature	22℃	Outlet	Outflow

Table 3 Grid independence test of flow velocity and average temperature in the train

Type	Cell number(million)	Flow velocity(m/s)	Average temperature (℃)
Grid 1	7.18	0.1502	20.78
Grid 2	12.80	0.1547	21.07
Grid 3	15.55	0.1530	21.01

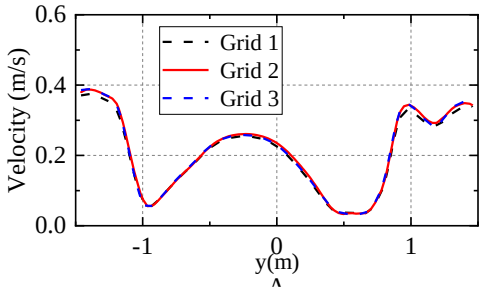

Fig. 3 Grid independence investigation

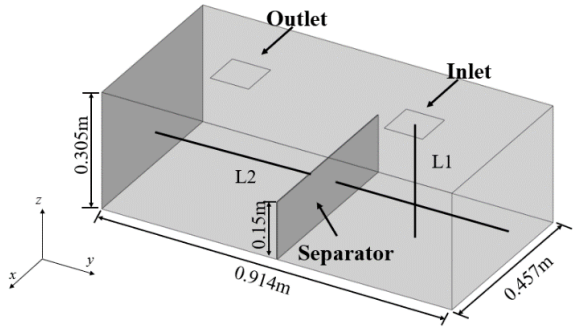

Fig. 4 Setup of validation case

million, respectively. Figure 3 shows that as the number of grids increases, the velocity distribution in the carriage is basically unchanged. Table 3 shows the independence investigation of the mean flow velocity and average temperature in the car, which shows that the number of grids has little effect on the overall velocity field and temperature field in the car. Therefore, the following numerical simulation is carried out with 12.80 million grids.

3.4 Numerical Validation

In order to validate the numerical method in this study, a model with a certain degree of similarity is established and numerically calculated, according to the experiments by Posner et al. (2003).

The model is shown in Fig. 4. The size of the model is 0.914 × 0.457 × 0.305 m, the dimensions of the air inlet and outlet are 0.1 × 0.1 m, and there is a partition in the center of the floor, with a height of 0.15 m. The air velocity is 0.235 m/s, the temperature is 15°C, and the outlet is set as outflow. The wall temperatures are all 15°C. Velocity measuring points were deployed at L1 and L2 to monitor velocity distribution.

According to Fig. 5 the numerical results and the experimental data are essentially the same, with a slight deviation for the two monitoring linear velocities of L1 and L2. In all, the numerical method in this study has good accuracy and reliability.

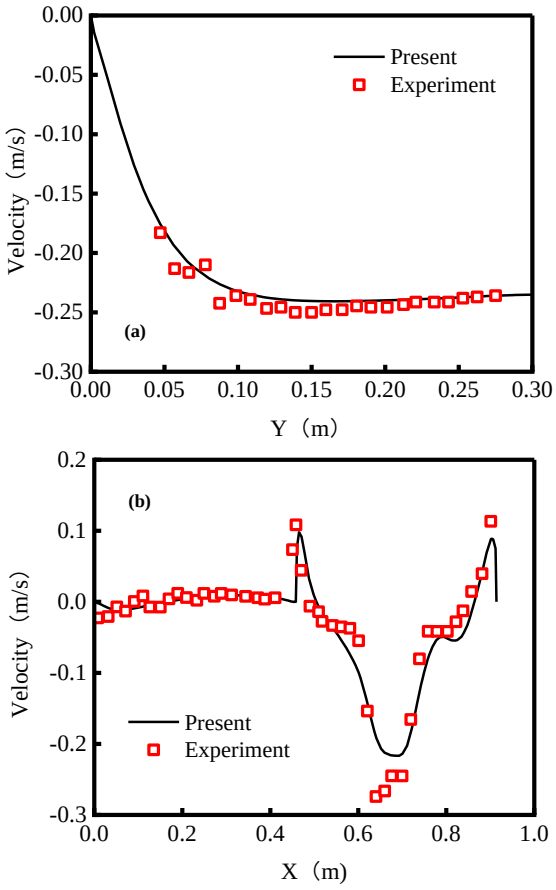

Fig. 5 Comparison of the results for validation from the numerical simulation and the experiment(a)Velocity in the L1 direction (b)Velocity in the L2 direction

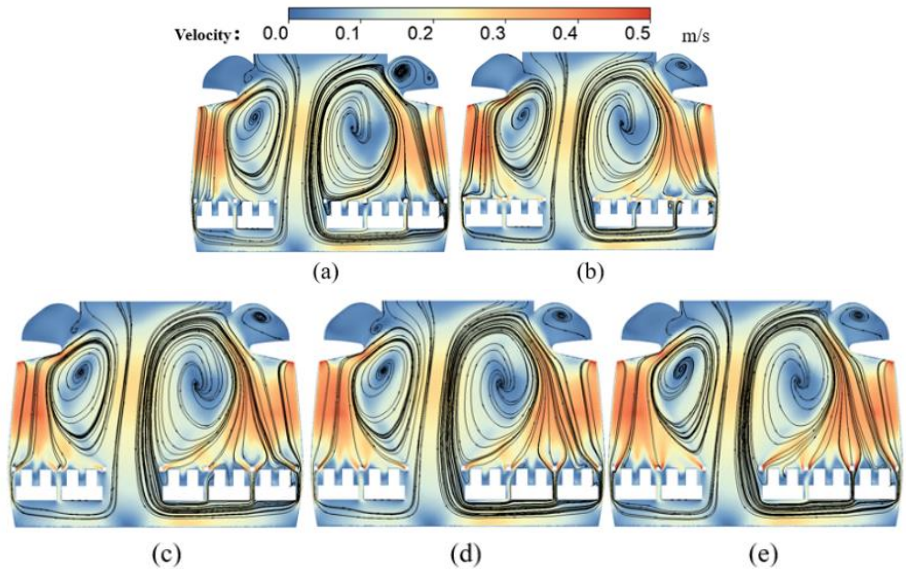

Fig. 6 Law of velocity flow field in the vertical direction (a)Case 1 (b)Case 2 (c)Case 3 (d)Case 4 (e)Case 5

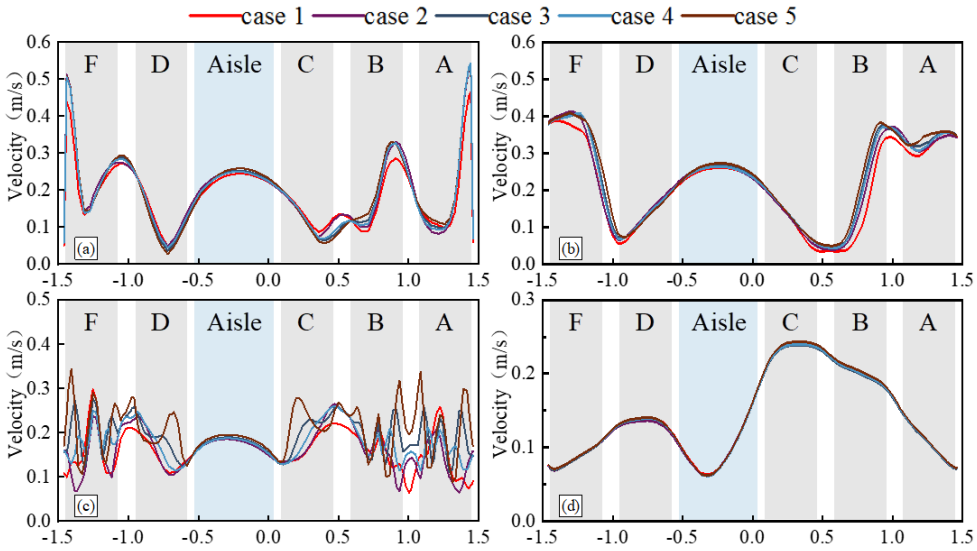

Fig. 7 Velocity profile(a)Velocity distribution at 1.7 m above the ground(b)Velocity distribution at 1.3 m above the ground(c)Velocity distribution at 0.7 m above the ground(d)Velocity distribution at 0.1 m above the ground

4. RESULTS AND DISCUSSION

A numerical method is used to simulate the flow characteristics of the vehicle under five different seat armrest ventilation cases. The advantages and disadvantages of each scheme are compared in four ways, being the flow field, temperature field, pollutant distribution and evaluation index.

4.1 Flow Field

Figure 6 shows the distribution of the velocity in the carriages under different air supply angles. Under the five cases, the airflow on the right side of the carriages is mainly moved to the upper part of the carriages under the combined action of the air outlet at the lower part of the luggage rack and the thermal plume of the human bodies. This interacts with the flow from the ceiling. Case 2, Case 4 and Case 5 all generate obvious vortices inside the carriage, which will lead to the accumulation of respiratory pollutants. In the lower part of the car, under the action of the flow field, the airflow blows from the left to the right and flows upward to complete the cycle. Two obvious vortices are produced, showing a symmetrical distribution.

Figure 7 shows the velocity distribution at different heights from the floor under the five cases. For a point 1.7 m above the ground, the airflow velocity increases, due to the action of the air outlet. Near the head of the human body, the speed is distributed between 0.05-0.4 m/s, and the speed fluctuations of the second and fourth options are relatively large, which may cause a feeling of wind on the faces of the people, causing discomfort. At the personalized air vents, the personalized air supply interacts with the airflow in the carriages, and there are obvious speed fluctuations, but the speed changes very little in all cases, only changing by between 0.1 and 0.3 m/s.

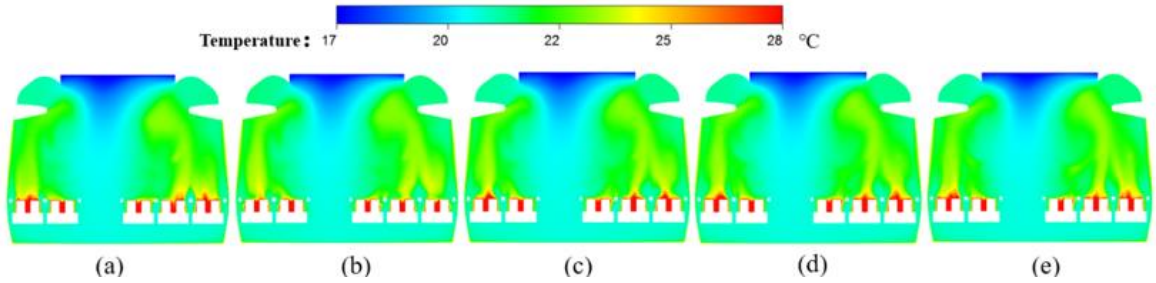

Fig. 8 Law of temperature in the vertical direction (a)Case 1 (b)Case 2 (c)Case 3 (d)Case 4 (e)Case 5

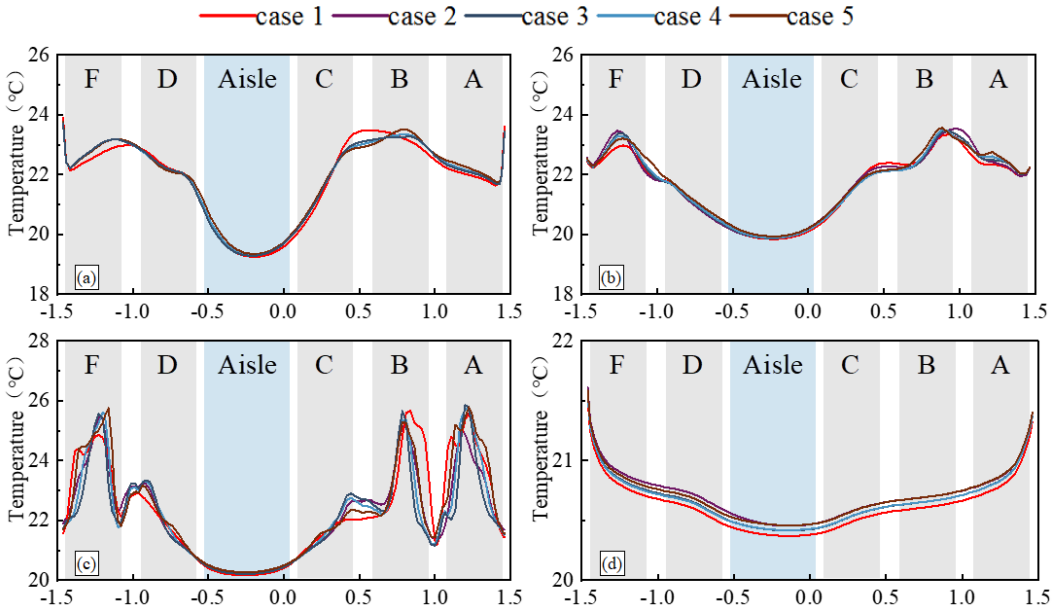

Fig. 9 Temperature profile (a)Temperature distribution at 1.7 m from the ground (b)Temperature distribution at 1.3 m from the ground (c)Temperature distribution at 0.7 m from the ground (d)Temperature distribution at 0.1 m from the ground

4.2 Temperature Distribution

Figure 9 shows the temperature distribution in the carriages under different cases. When the personalized ventilation system is not used, the temperature inside the carriages is relatively low. When using a personalized ventilation system, the temperature around the passenger is higher, which can enhance the effect of the body thermal plume and accelerate the rise of the air flow. All five cases showed obvious temperature stratification. Taking the seat as the boundary, the lower body temperature is lower, the upper body temperature is higher.

Figure 9 shows the temperature distribution at different heights from the ground. There is temperature fluctuation at 1.7 m from the ground. At a distance of 1.3 m from the ground, in the five cases, the temperature changes near a single passenger are all less than 3°C, which meets the requirements of human thermal comfort. The temperature fluctuation near the human body is mainly due to human body temperature. The human leg is 0.1 m away from the ground. As shown in Fig. 8 (d), the temperature is relatively stable and has no obvious fluctuation, showing that the personalized ventilation system does not affect the temperature distribution in the carriage.

4.3 Pollutant Distribution

In order to study the transmission law of respiratory pollutants of the passengers during the use of the personalized air supply system, a plane 10 cm in front of the passengers was taken as the research plane.

First, the respiratory pollutants of the five passengers in the 9th row are individually marked, to study the flow state of the respiratory pollutants. As shown in Fig. 10, the case in which the personalized ventilation system is not used, and the case in which the personalized ventilation angle is 45°, are compared. Under both cases, the respiratory pollutants produced by passenger A will move to the upper part of the carriages along with the airflow. When personalized ventilation is not used, the respiratory pollutants of passengers B, C, D, and F will accumulate in the passenger breathing area and spread around, which may lead to problems, such as higher concentrations of pollutants in the breathing area of other passengers. When using personalized ventilation, the respiratory pollutants of passengers B, C, and F will flow to the upper part of the

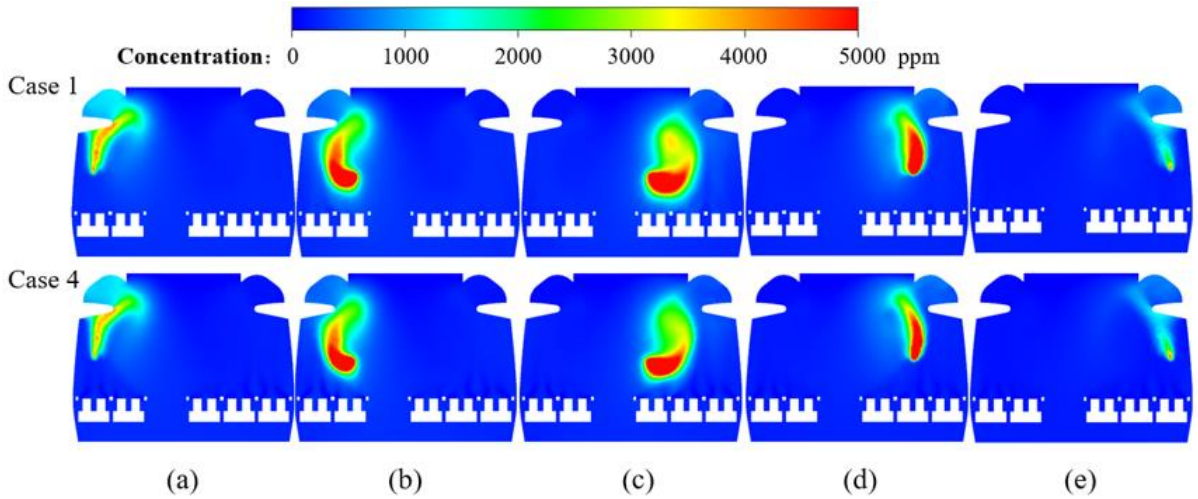

Fig. 10 Case 1 and Case 4 distribution of respiratory pollutants by passengers (a)passenger F(b)passenger D (c)passenger C (d)passenger B (e)passenger A

Table 4 Percentage reduction of pollutants in exposure region

angle	Passenger A	Passenger B	Passenger C	Passenger D	Passenger F	Average value
0°	15.52%	16.93%	13.48%	13.1%	18.68%	15.84%
30°	17.51%	23.7%	14.15%	12.54%	23.65%	19.27%
45°	19.19%	25.6%	13.57%	11.84%	22.65%	19.76%
60°	17.04%	28.75%	11.91%	10.69%	21.46%	19.68%

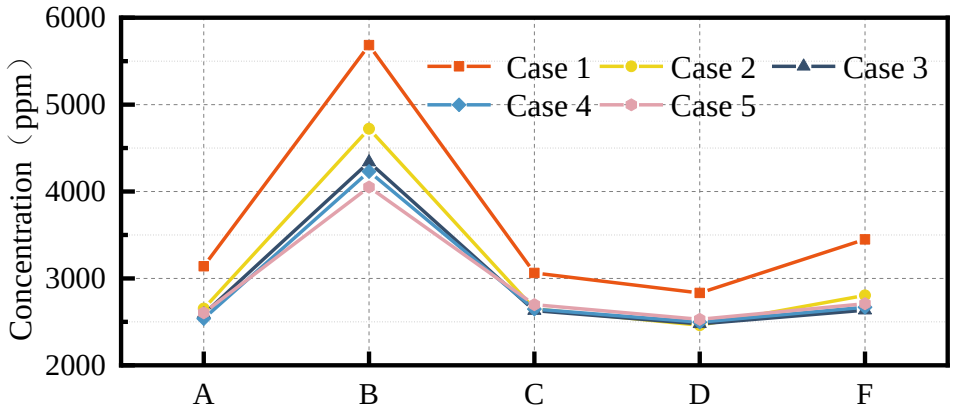

Fig. 11 Average pollutant concentration in the breathing zone of a typical passenger

carriages with the airflow, reducing the tendency to spread around. As for passenger D, although it also accumulates in the passenger exposure region, it does not affect the surrounding passengers. Nine planes of 300 × 300 mm were taken as the exposure region of five passengers, and the average CO_2 concentration on the nine planes was taken as the pollutant concentration in the exposure region of the passengers. Figure 11 shows the pollutant concentrations in the passenger exposure region. When the personalized air supply angles are 0°, 30°, 45°, and 60°, the pollutant concentration in the passenger exposure region is always lower than that of the no personalized ventilation case. When the comfort problem is not considered, these four cases can meet the requirements of According to Table 4, when personalized ventilation is adopted, the fluctuation amplitudes of pollutants in the passenger breathing zone are 15.84%, 19.27%, 19.76% and 19.68%, respectively, compared with the original ventilation system. For Passenger B, the personalized ventilation system blocked the respiratory pollutants from passenger C and allowed the respiratory pollutants from passenger B to flow up the carriage. With the increase in air supply angle, the concentration of pollutants in the respiratory area decreased. The results show that for case 5, the concentration in the respiratory area was the lowest, being 28.75% lower than case 1. During the epidemic period, while meeting the requirements of epidemic prevention and control, the mean non-uniform coefficient also needs to be considered, to select the optimal case.

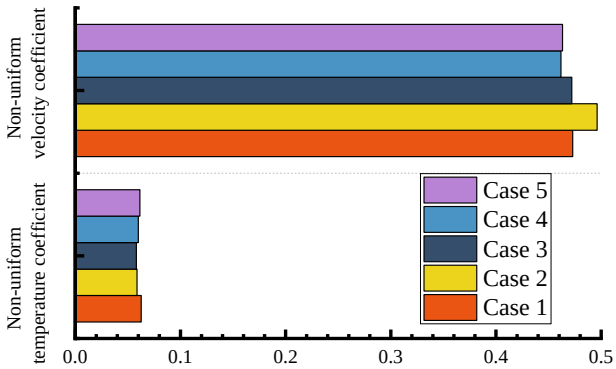

Fig. 12 Mean non-uniform coefficient under different cases

4.4 Evaluation Indicators

Figure 12 shows the mean non-uniform coefficient in the carriages of the five cases. When the personalized ventilation system is used, the mean non-uniform coefficient in the carriage will change, but the change is large, mainly because the supply angle of the personalized ventilation only changes under different working conditions, and this has little effect on the overall air distribution in the carriage. The data shows that for case 2, the mean non-uniform velocity coefficient will increase by 4.8%, indicating that the comfort of the passengers may be affected when the personalized ventilation system is used improperly. For case 4, the mean non-uniform velocity coefficient in the carriage will decrease by 2.3%. For case 3, the decrease in percentage of the mean non-uniform coefficient is 7.28%, and the decreasing percentage of the mean non-uniform velocity coefficient is 2.37%. If air supply angle is reasonable, it can effectively improve the uniformity of the flow field and the thermal comfort of passengers. When the air supply angle is appropriate, it can effectively reduce the pollutant concentration and improve the smoothness and uniformity in the carriage, such that the performance of the system is better than that of the control case.

5. CONCLUSION

In this paper, a numerical model of a high-speed train carriage is established, and the tracer gas method is used to study the effect of different air supply angles on the performance of a seat armrest embedded personalized ventilation system. The main conclusions are as follows

(1) The personalized ventilation system in the armrest of the carriage seat can effectively reduce the average pollutant concentration in the passenger exposure region, and can improve the airflow uniformity in the carriage, improving thermal comfort.

(2) With the increase of air supply angle, the average concentration of respiratory pollutants in the breathing area of passengers of column B decreased significantly, the largest decrease being 28.75%. The other four columns had a similar percentage reduction in the average respiratory pollutant concentration.

(3) For case 4, the pollutant concentration in the passenger's exposure region is the lowest and the air flow uniformity is better, so this can be used as a reference in the design of personalized ventilation systems.

This paper mainly focuses on the effect of different air supply angles on the performance of personalized ventilation systems. A limitation is that the transient respiratory flow was not simulated. The research results can provide some reference for epidemic prevention and control, in train carriages.

ACKNOWLEDGEMENT

This work was supported by National Natural Science Foundation of China (No. 12172308), Fundamental Research Funds for the Central Universities (2682021ZTPY124) and and State Key Laboratory of Traction Power (2023TPL-T06).

CONFLICT OF INTEREST

The authors declare that they have no known competing financial interests or personal relationships that could have appeared to influence the work reported in this paper.

AUTHORS CONTRIBUTION

Xin Liu: Methodology, Software, Writing – Original Draft. Tian Li: Conceptualization, Investigation, Writing – Reviewing and Editing. Songbo Wu: Writing –Editing, Validation. Jiye Zhang: Funding acquisition, Resources.

REFERENCES

Ai, Z. T., Mak, C. M., Gao, N. P., & Niu, J. L. (2020). Tracer gas is a suitable surrogate of exhaled droplet nuclei for studying airborne transmission in the built environment. *Building Simulation*, 13(3), 489-496. https://doi.org/10.1007/s12273-020-0614-5

Assaad, D. A., Ghali, K., & Ghaddar, N. (2019). Effect of flow disturbance induced by walking on the performance of personalized ventilation coupled with mixing ventilation. *Build and Environment* 160, 106217.1-106217.18. https://doi.org/10.1016/j.buildenv.2019.106217

Alain, M., Kamel, G., & Nesreen, G. (2015). Low-mixing coaxial nozzle for effective personalized ventilation. *Indoor and Built Environment* 24(2), 225-243. https://doi.org/10.1177/1420326X13508967

Barone, G., Buonomano, A., Forzano Cesare., & Palombo, A. (2020). Enhancing trains envelope - heating, ventilation, and air conditioning systems: A new dynamic simulation approach for energy, economic, environmental impact and thermal comfort analyses. *Energy*, 204. https://doi.org/10.1016/j.energy.2020.117833

Mboreha, C. A., Sun, J., Wang, Y., & Sun, Z. (2022). Airflow and contaminant transport in innovative personalized ventilation systems for aircraft cabins:

A numerical study. *Science and Technology for the Built Environment* 28(4), 557-574. https://doi.org/10.1080/23744731.2022.2050632

Chen, Q. (1995). Comparison of different k-epsilon models for indoor air-flow computations. *Numerical Heat Transfer, Part B*, 28(3), 353-369. https://doi.org/10.1080/10407799508928838

Debnath, S., Saha, A. K., Siddheshwar, P. G., & Roy, A. K. (2018). On dispersion of a reactive solute in a pulsatile flow of a two-fluid model. *Journal of Applied Fluid Mechanics*, 12(3), 987-1000. https://doi.org/10.29252/jafm.12.03.29101

Elvire, K., Nesreen, G., Kamel, G., Douss A., & Saud, G. (2021). Effect of individually controlled personalized ventilation on cross-contamination due to respiratory activities. *Build and Environment*, 194. https://doi.org/10.1016/j.buildenv.2021.107719

Ghaddar, D., Itani, M., Ghaddar, N., Ghali, K., & Zeaiter, J. (2021). Model-based adaptive controller for personalized ventilation and thermal comfort in naturally ventilated spaces. *Building Simulation*, 14(6), 1757-1771. https://doi.org/10.1007/s12273-021-0783-x

Gupta, J. K., Lin, C. H., & Chen, Q. Y. (2009). Flow dynamics and characterization of a cough. *Indoor Air*, 19(6), 517-525. https://doi.org/10.1111/j.1600-0668.2009.00619.x

Gupta, J. K., Lin, C. H., & Chen, Q. Y. (2010). Characterizing exhaled airflow from breathing and talking. *Indoor Air*, 20(1), 31-39. https://doi.org/10.1111/j.1600-0668.2009.00623.x

Hachem, M., Saleh, N., Paunescu, A., Momas, I., Bensefa-Colas, L. (2019). Exposure to traffic air pollutants in taxicabs and acute adverse respiratory effects: A systematic review. *Science of the Total Environment*, 693, 133439. https://doi.org/10.1016/j.scitotenv.2019.07.245

Liu, H., He, S. D., Shen, L., & Hong, J. R. (2021). Simulation-based study of COVID-19 outbreak associated with air-conditioning in a restaurant. *Physics of Fluids* 33(2), 023301. https://doi.org/10.1063/5.0040188

Izadyar, N., & Miller, W. (2022). Ventilation strategies and design impacts on indoor airborne transmission: A review. *Building and Environment*, 218, 109158. https://doi.org/10.1016/j.buildenv.2022.109158

Li, X. P., Niu, J. L., & Gao, N. P. (2011). Spatial distribution of human respiratory droplet residuals and exposure risk for the co-occupant under different ventilation methods. *HVAC & R Research*, 17(4), 432-445. https://doi.org/10.1080/10789669.2011.578699

Li, X. P., Niu, J. L., & Gao, N. P. (2013). Co-occupant's exposure to exhaled pollutants with two types of personalized ventilation strategies under mixing and displacement ventilation systems. *Indoor Air*, 23(2), 162-171. https://doi.org/10.1111/ina.12005

Li, X. D., Shang, Y. D., Yan, Y. H., Yang, L., & Tu, J. Y. (2018). Modelling of evaporation of cough droplets in inhomogeneous humidity fields using the multi-component Eulerian-Lagrangian approach. *Building and Environment*, 128, 68-76. https://doi.org/10.1016/j.buildenv.2017.11.025

Li, T., Wu, S. B., Yi, C., Zhang, J. Y., & Zhang, W. H. (2022). Diffusion characteristics and risk assessment of respiratory pollutants in high-speed train s. *Journal of Wind Engineering and Industrial Aerodynamics*, 222. https://doi.org/10.1016/j.jweia.2022.104930

Li, M. X., Zhao, B., Tu, J. Y., & Yan, Y. H. (2015). Study on the carbon dioxide lockup phenomenon in aircraft cabin by computational fluid dynamics. *Building Simulation* 8(4), 431-441. https://doi.org/10.1007/s12273-015-0217-8

Mangili, A., & Gendreav, M. A. (2005). Transmission of infectious diseases during commercial air travel. *The Lancet* (North American Edition), 365(9463), 989-996. https://doi.org/10.1016/S0140-6736(05)71089-8

Mao, N., Yu, H., Zhuang, J. J., & Song, M. J. (2022). Numerical study on supply parameters' influence on ventilation performance of a personalized air conditioning system for sleeping environments. *Journal of Thermal Analysis and Calorimetry*, 147(20), 11331-11343. https://doi.org/10.1007/s10973-022-11332-5

Mechighel, F., Armour, N., & Dost, S. (2021). Modeling of the effect of the presence of a free surface on transport structures and mixing during the dissolution process of silicon into germanium melt. *Journal of Thermal Analysis and Calorimetry*, 146(1), 61-91. https://doi.org/10.1007/s10973-020-09957-5

Melikov, A. K. (2004). Personalized ventilation. *Indoor Air*, 14(7), 157-167. https://doi.org/10.1111/j.1600-0668.2004.00284.x

Melikov, A. K., Ivanova, T., & Stefanova, G. (2012). Seat headrest-incorporated personalized ventilation: Thermal comfort and inhaled air quality. *Build and Environment*, 47(1), 100-108. https://doi.org/10.1016/j.buildenv.2011.07.013

Pesic, D. J., Zigar, D. N., Anghel, I., & Glisovic, S. M. (2016). Large eddy simulation of wind flow impact on fire induced indoor and outdoor air pollution in an idealized street canyon. *Journal of Wind Engineering and Industrial Aerodynamics*, 155, 89-99. https://doi.org/10.1016/j.jweia.2016.05.005

Posner, J. D., Buchanan, C. R., & Dunn-Rankin, D. (2003). Measurement and prediction of indoor air flow in a model room. *Energy and Buildings*, 35(5), 515-526. https://doi.org/10.1016/S0378-7788(02)00163-9

Razvan, M., Georgescu, M. R., Meslem, A., Nastase, I., & Bode, F. (2021). Personalized ventilation solutions for reducing CO2 levels in the crew quarters of the

International Space Station. *Build and Environment*, 204. https://doi.org/10.1016/j.buildenv.2021.108150

Sen, N. (2021). Transmission and evaporation of cough droplets in an elevator: Numerical simulations of some possible scenarios. *Physics of Fluids*, 33(3), 033311. https://doi.org/10.1063/5.0039559

Shih, T. H., Zhu, J., & Lumley, J. L. (1995). A new reynolds stress algebraic equation model. *Computer Methods in Applied Mechanics and Engineering*, 125(1-4), 287-302. https://doi.org/10.1016/0045-7825(95)00796-4

Sherman, M .H. (1990). Tracer-gas techniques for measuring ventilation in a single zone. *Build and Environment*, 25(4), 365-374. https://doi.org/10.1016/0360-1323(90)90010-O

Wang, H. T., Lin, M. D., & Chen, Y. (2014). Performance evaluation of air distribution systems in three different china railway high-speed train cabins using numerical simulation. *Building Simulation*, 7(6), 629-638. https://doi.org/10.1007/s12273-014-0168-5

Wei, J. J., & Li, Y.G. (2015). Enhanced spread of expiratory droplets by turbulence in a cough jet. *Building and Environment*, 93(P2), 86-96. https://doi.org/10.1016/j.buildenv.2015.06.018

Wu, S. B., Li, T., Yi, C., Zhang, J. Y., & Zhang, W. H. (2022). Effects of exhaust methods on air distribution and respiratory pollutants diffusion characteristics in high-speed train compartments (in Chinese). *Sci Sin Tech*, 52. https://doi.org/10.1360/SST-2021-0363

Xu, C. W., Wei, X. X., Liu, L., Su, L., Liu, W. B., Wang, Y., Nielsen, P. V. (2020). Effects of personalized ventilation interventions on airborne infection risk and transmission between occupants. *Build and Environment* 180, 107008. https://doi.org/10.1016/j.buildenv.2020.107008

Xu, C. W., Nielsen, P. V., Liu, L. L., Jensen, R. L., & Gong, G. C. (2018). Impacts of airflow interactions with thermal boundary layer on performance of personalized ventilation. *Build and Environment*, 135, 31-41. https://doi.org/10.1016/j.buildenv.2018.02.048

Xu, J. C., Fu, S., & Chao, C. Y. H. (2021). Performance of airflow distance from personalized ventilation on personal exposure to airborne droplets from different orientations. *Indoor and Built Environment*, 30(10), 1643-1653. https://doi.org/10.1177/1420326X20951245

Xui, J. C., Fu, S. C., & Christopher, Y. H C. (2021). Performance of airflow distance from personalized ventilation on personal exposure to airborne droplets from different orientations. *Indoor and Built Environment*, 30(10), 1643-1653.

Yang, C. Q., Yang, X. D., & Zhao, B. (2015). The ventilation needed to control thermal plume and particle dispersion from manikins in a unidirectional ventilated protective isolation room. *Building Simulation*, 8(5), 551-565. https://doi.org/10.1007/s12273-014-0227-6

Zhang, L., & Li, Y. G. (2021). Dispersion of coughing droplets in a fully-occupied high-speed rail cabin. *Build and Environment*, 47(1), 58-66. https://doi.org/10.1016/j.buildenv.2011.03.015

Zhang, T. F., Li, P. H., & Wang, S. G. (2012). A personal air distribution system with air terminals embedded in chair armrests on commercial airplanes. *Build and Environment*, 47, 89-99. https://doi.org/10.1016/j.buildenv.2011.04.035

Zhou, Y., Wang, M. Y., Wang, M. N., & Wang, Y. (2018). Predictive accuracy of Boussinesq approximation in opposed mixed convection with a high-temperature heat source inside a building. *Building and Environment*, 144, 349-356. https://doi.org/10.1016/j.buildenv.2018.08.043